Large nonlinear magneto-optical effect in the centrosymmetric ferromagnetic semiconductor EuO

Masakazu Matsubara,[1,*] Andreas Schmehl,[2] Jochen Mannhart,[2] Darrell G. Schlom,[3] and Manfred Fiebig[1]
[1]*HISKP, Universität Bonn, Nussallee 14-16, 53115 Bonn, Germany*
[2]*Institut für Physik, Universität Augsburg, Augsburg 86135, Germany*
[3]*Department of Materials Science and Engineering, Cornell University, Ithaca, New York 14853-1501, USA*
(Received 13 April 2010; revised manuscript received 1 June 2010; published 30 June 2010)

Pronounced magnetic-dipole-induced second-harmonic generation (SHG) is observed in epitaxial films of the ferromagnetic semiconductor EuO. The SHG light wave emerges background-free at the Curie temperature and couples linearly to the spontaneous magnetization. The SHG spectrum is determined by spin-allowed and spin-forbidden transitions between the $4f$ ground state and the $5d(t_{2g})$ states of the Eu^{2+} ion. At the coercive field, components of the spontaneous magnetization perpendicular to the applied field are observed. Spatially resolved hysteresis measurements reveal that the ferromagnetic domains possess an average extension of <1 μm although pinning effects can stabilize domains that are two orders of magnitude larger.

DOI: 10.1103/PhysRevB.81.214447 PACS number(s): 75.50.Pp, 42.65.Ky, 78.20.Ls, 75.47.Lx

Europium oxide (EuO) belongs to the small group of ferromagnetic semiconductors. It has been investigated extensively since its discovery in the 1960s (Refs. 1 and 2) because of a multitude of remarkable properties such as an insulator-metal transition,[3] colossal magnetoresistance,[4,5] threefold enhancement of the ferromagnetic ordering temperature,[6] and nearly 100% spin polarization in the ferromagnetic state.[7–10] Recently the interest in EuO as a spintronics material has experienced a remarkable boost. The possibility to produce high-quality epitaxial films of EuO with special capping layers that are stable under ambient conditions has made a broad range of functionalities accessible.[9,11] Usually these involve spatial patterning or the controlled introduction of local inhomogeneities into the EuO heterostructures. In contrast, if homogeneity is required, fluctuations in the local properties are to be avoided. Therefore, the development of techniques that probe the *local* properties of EuO-based structures is desirable because available techniques such as transport and diffraction measurements only probe the average response of the whole sample. Linear optical techniques such as Faraday and Kerr rotation can be used to probe the magnetization of the europium chalcogenides EuX (X=O, S, Se, and Te) locally.[12,13] Nonlinear optical techniques, however, offer higher spectral resolution, detect long-range order background-free, and are capable of distinguishing even subtle nuances in the ferroic structure.[14,15] Pronounced nonlinear optical effects were recently reported for EuSe and EuTe films.[16] EuO has not been characterized by nonlinear optical techniques. Yet, based on the aforementioned issues it may be the compound with the most outstanding properties in the EuX series.

Here we report the spectrally and spatially resolved investigation of epitaxial EuO films by optical second-harmonic generation (SHG). Even though EuO has a *centrosymmetric* crystal structure which prevents leading-order contributions to SHG, a pronounced SHG light wave is emitted. It emerges background-free at the Curie temperature and is therefore purely ferromagnetic in origin, coupling linearly to the magnetization. Spectroscopy reveals the microscopic origin of the large SHG yield. Field-dependent measurements reveal a magnetic hysteresis with additional magnetization components in the vicinity of the coercive field. SHG imaging experiments reveal a network of subresolution ferromagnetic domains interspersed with pinned regions of larger expansion.

EuO has a centrosymmetric cubic rocksalt structure (point group $m3m$), as shown in Fig. 1(a). The stoichiometric compound is a paramagnetic semiconductor with a band gap of $\sim$1.2 eV at room temperature. It undergoes a ferromagnetic transition at T_C=69 K, below which it has the magnetic point symmetry $4/m$. The Eu^{2+} ions have localized $4f^7$ electrons with $^8S_{7/2}$ as the ground state. The electronic structure of EuO has intensively been investigated in experimental and theoretical studies.[2] The lowest excitations in the near-infrared and visible regions have been assigned to the transitions from the $4f^7$ ground state to the $5d(t_{2g})$ orbitals.

In the majority of cases, SHG is applied to noncentrosymmetric materials or to the surface or interface of centrosymmetric materials where the inversion symmetry is locally broken by the discontinuity.[14,15] In this case SHG is dominated by electric-dipole (ED) transitions between the electronic states. In centrosymmetric systems, however, SHG is only allowed if higher-order multipole contributions in the expansion of the electromagnetic light field like magnetic-dipole (MD) or electric-quadrupole (EQ) contributions are involved. In the EuX compounds this leads to[16,17]

$$P_i(2\omega) = \epsilon_0(\chi_{ijk}^{\mathrm{cr}} + \chi_{ijk}^{\mathrm{mag}})E_j(\omega)H_k(\omega), \qquad (1)$$

where χ_{ijk}^{cr} and $\chi_{ijk}^{\mathrm{mag}}$ are the second-order nonlinear susceptibilities related to crystallographic (paramagnetic) SHG and to magnetization-induced SHG, respectively. Note that we refrain from writing the latter as $\chi_{ijkl}H_l(0)$ with $\vec{H}(0)$ as externally applied field[16] since this may incorrectly imply that the external field instead of a spontaneous magnetization is responsible for the magnetization-induced SHG. The external field merely enhances the SHG yield by promoting a single-domain state and its relation to the magnetization is ambiguous because of the hysteresis. $E_j(\omega)$ and $H_k(\omega)$ in Eq. (1) denote the j-polarized electric field ($\sim$ED) and the

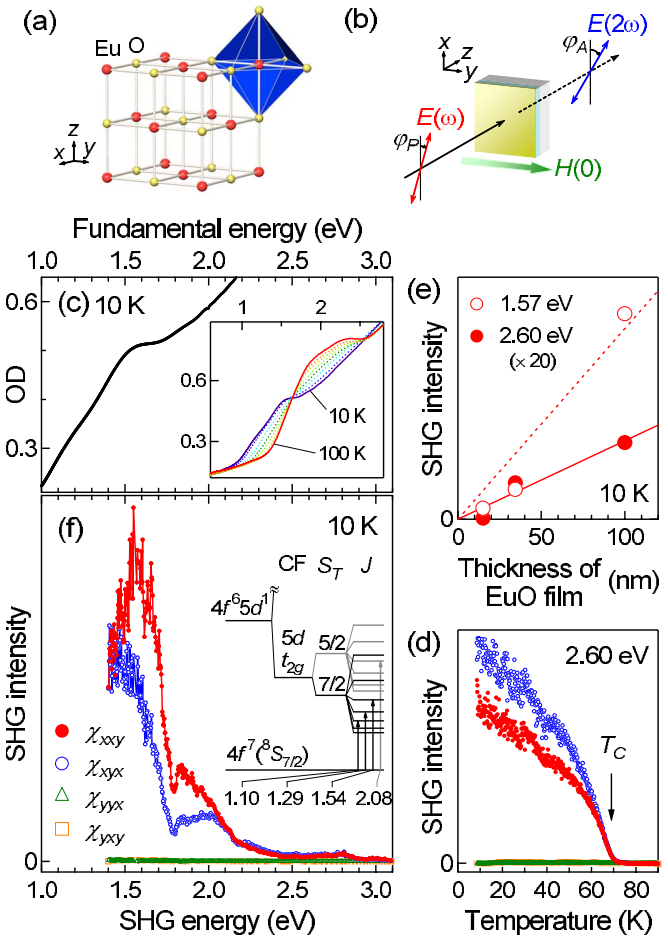

FIG. 1. (Color online) Linear and nonlinear optical spectroscopy on epitaxial EuO(001) films. (a) Crystal structure of EuO. (b) Experimental configuration of the SHG measurements. (c) Spectrum of the optical density (OD) at 10 K of a-Si/EuO/$YAlO_3$ obtained with unpolarized incident light. The inset shows the temperature variation at 10, 30, 50, 60, 65, 70, 80, and 100 K. (d) Temperature dependence of the SHG intensity with assignments of SHG tensor components as in (f). (e) Thickness dependence of the SHG intensity at 10 K for χ_{xxy} at $2\hbar\omega$=1.57 and 2.60 eV. (f) SHG spectra for different polarization configurations of the incident fundamental and the detected component of the SHG light. The inset shows the electronic energy levels of the Eu^{2+} ion (Ref. 22). CF and S_T denote crystal field and total spin, respectively. SHG data were taken on a ferromagnetic single-domain sample ($\mu_0 H_y$=0.1 T).

k-polarized magnetic field (~MD) of the fundamental light, respectively, that induce the i-polarized SHG wave $P_i(2\omega)$(~ED).

The EuO films are probed with light incident along one of the principal axes ($k \| z$). For this configuration, the nonzero SHG tensor components for different directions of the spontaneous magnetization are summarized in Table I.[18] With $k \| z$ any crystallographic SHG for the configurations discussed here are zero so that the magnetically induced SHG signal is expected to emerge free of background. We thus replace $\chi_{ijk}^{\mathrm{mag}}$ by χ_{ijk} in the following. Note that surface-induced noncentrosymmetric ED-SHG leads to the same polarization selection rules as bulk-induced centrosymmetric MD-SHG.[18] Surface contributions can, however, be excluded because of the

TABLE I. Nonzero tensor components for magnetization-induced bulk magnetic-dipole SHG in ferromagnetic EuO. These are derived by considering $4/m$ as the magnetic point group symmetry with a spontaneous magnetization parallel to one of the principal axes with light incident along the z axis (Ref. 18).

	Bulk MD-SHG $P_i(2\omega)=\epsilon_0\chi_{ijk}E_j(\omega)H_k(\omega)$
$M \| x$	χ_{yyx}, χ_{yxy}, χ_{xyy}, χ_{xxx}
$M \| y$	χ_{xxy}, χ_{xyx}, χ_{yxx}, χ_{yyy}
$M \| z$	

dependence of the SHG yield on the thickness of the EuO films, as shown below. EQ contributions are neglected because they are much smaller than the MD contributions[19] and were not detected in our experiment. Moreover, our substrate, $YAlO_3$, is centrosymmetric (point group mmm) and nonmagnetic and it was verified that it does not contribute to the present SHG signal.

Epitaxial EuO(001) films with oxygen vacancies of $<0.1\%$ were grown on a two-side polished $YAlO_3$(110) substrate by molecular-beam epitaxy.[9] For most of the measurements film with a thickness of 100 nm were used for which growth-related magnetostrictive effects can be neglected. For preventing degradation in air, the films were protected by an amorphous silicon (a-Si) cap layer of 10 nm. For the SHG measurements, a regenerative Ti:sapphire amplifier system with a central wavelength of 800 nm (1.55 eV), a pulse width of 120 fs, and a repetition rate of 1 kHz was used as the light source. Unless otherwise stated, the SHG spectra were measured in transmission in an external magnetic field of 0.1 T applied in the Voigt configuration ($H \| y$), as shown in Fig. 1(b). The EuO sample was excited by light with a photon energy $\hbar\omega$ of 0.67–1.56 eV generated by an optical parametric amplifier. The fundamental light was incident onto the a-Si-covered side of the sample so that the SHG light generated in the EuO was not absorbed by the a-Si. The pulse energy and focus diameter were chosen as ~1 μJ and ~400 μm, respectively. A polarizer, a wave plate, and long-pass filters were used to set the polarization φ_P of the incoming fundamental light and to block higher harmonics generated in the optical components. The SHG light was separated from the incident fundamental light by short-pass filters and a monochromator and detected with a photomultiplier tube. The polarization φ_A of the SHG light was analyzed by a polarization filter. The SHG spectra were normalized to spectral beam variations using the spectrally flat SHG response of a silver mirror. They were also normalized to the spectral response of the detection system. For the spatially resolved measurements, a liquid-nitrogen-cooled digital camera was used as the detector.

Figure 1(c) shows the linear absorption spectrum of the a-Si/EuO/$YAlO_3$ sample at 10 K obtained with unpolarized incident light. The structures in the region of 1.0–1.7 eV are attributed to the $4f \rightarrow 5d(t_{2g})$ transitions of the EuO. The slope of the absorption spectrum beyond 1.7 eV is caused by the absorption of a-Si.[20] The large temperature-dependent spectral shift of the absorption shown in the inset of Fig. 1(c) is due to the exchange splitting between the

spin-up and spin-down states of the $5d$ orbitals.[21] The bulk-like linear optical properties of the EuO films as well as the good crystallographic and transport properties[9] confirm the excellent quality of the epitaxial EuO.

Figure 1(d) shows the temperature and polarization dependence of the SHG intensity. For suppressing any modification of the SHG signal by the temperature dependence of the absorption in the inset of Fig. 1(c), the SHG data were, in spite of the lower SHG yield, taken at $2\hbar\omega=2.60$ eV, where the absorption is temperature independent. Although SHG in the ED approximation is forbidden due to the centrosymmetry, surprisingly, pronounced SHG signals are observed below T_C. Taking the ED-SHG yield of GaAs as Ref. 16 the magnitude of the MD-SHG signal from EuO is two orders of magnitude higher than expected. The SHG signal disappears exactly at T_C which confirms its purely ferromagnetic origin. Neither crystallographic SHG from the EuO nor SHG from the a-Si and the $YAlO_3$ substrate contribute to the net signal which reveals SHG to be a background-free probe of the magnetic state of the EuO in the a-Si/EuO/$YAlO_3$ heterostructure. This contrasts with the work on EuSe and EuTe films where a SHG signal not coupling to the magnetic order was present, presumably because of the (111) orientation of the corresponding films.[16] In Fig. 1(d) χ_{xxy} and χ_{xyx} contribute to magnetically induced SHG whereas no signal is obtained from χ_{yyx} and χ_{yxy}. This is in agreement with Table I for a magnetization pointing along the y axis.

As mentioned, surface-induced noncentrosymmetric ED-SHG leads to the same polarization selection rules as bulk-induced centrosymmetric MD-SHG. In order to verify the origin of the SHG signal, we determined the dependence of the SHG intensity on the thickness of the EuO film at 1.57 eV (maximum SHG yield) and at 2.60 eV (our standard SHG probe energy) for the χ_{xxy} component at 10 K. The linear dependence revealed by Fig. 1(e) confirms that SHG in EuO is described by the bulk-induced MD process in Eq. (1).

For a more comprehensive analysis the polarization-dependent measurements in Fig. 2 were conducted. In Figs. 2(a) and 2(b) the polarization of one light beam (fundamental or SHG) is fixed while the other polarization is rotated. In Figs. 2(c) and 2(d) both polarizations are rotated with a fixed polarization difference between the ingoing fundamental light and the component of the outgoing SHG light that is detected.

If all four tensor components in Table I for $M\|y$ are taken into account, we calculate that the dependence of the SHG intensity on the analyzer angle $I(2\omega,\varphi_A)$ is proportional to $|\chi_{xxy}\cos\varphi_A|^2$ for $\varphi_P=0°$ and proportional to $|\chi_{xyx}\cos\varphi_A|^2$ for $\varphi_P=90°$. The dependence of the SHG intensity on the polarizer angle $I(2\omega,\varphi_P)$ at $\varphi_A=90°$ is proportional to $|\chi_{y\rho\rho}\sin 2\varphi_P|^2$ in which $\chi_{y\rho\rho}=\chi_{yyy}-\chi_{yxx}$. If the polarization of the fundamental and of the detected SHG contribution are rotated simultaneously, the SHG intensity for $\varphi_A=\varphi_P[E(2\omega)\|E(\omega)]$ and for $\varphi_A=\varphi_P+90°[E(2\omega)\perp E(\omega)]$ can be written as follows:

$$I_{\|}(2\omega,\varphi_A)\propto[(3\chi_{xxy}-\chi_{xyx}+\chi_{y\rho\rho})\cos\varphi_A + (\chi_{xxy}+\chi_{xyx}-\chi_{y\rho\rho})\cos 3\varphi_A]^2, \quad (2)$$

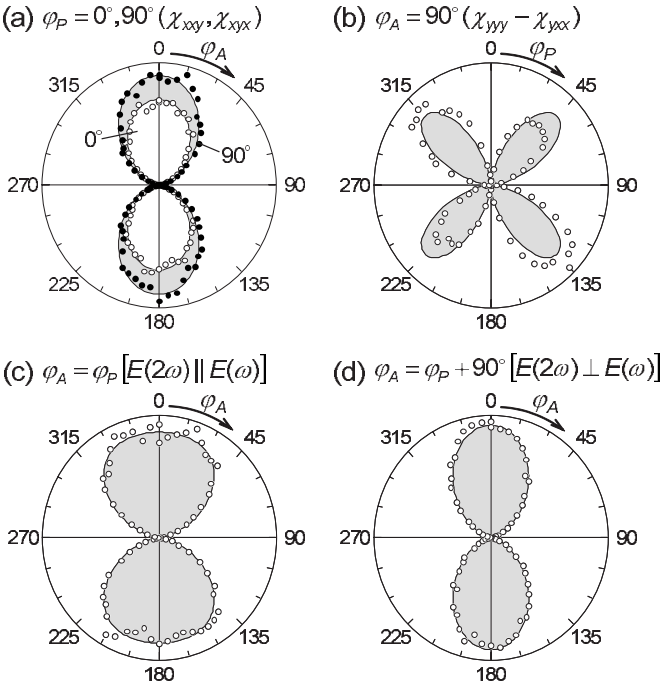

FIG. 2. Investigation of the SHG tensor components in Table I by anisotropy measurements at 10 K at $2\hbar\omega=2.60$ eV. Angles φ_P and φ_A denote the polarization of the incident fundamental light and the detected component of the SHG light, respectively, according to Fig. 1(b). Angles 0° and 90° correspond to the x and the y axes, respectively. The center of each polar diagram corresponds to zero. Solid lines represent fits to the equations mentioned in the text.

$$I_{\perp}(2\omega,\varphi_A)\propto[(\chi_{xxy}-3\chi_{xyx}-\chi_{y\rho\rho})\cos\varphi_A - (\chi_{xxy}+\chi_{xyx}-\chi_{y\rho\rho})\cos 3\varphi_A]^2. \quad (3)$$

Figure 2 reveals that in all cases good agreement is obtained between the experimental data and the fits even when a single set of fit parameters is assumed for all five configurations that were probed. We find that at our reference probe energy of 2.60 eV the magnitude of χ_{xxy} and χ_{xyx} is one order of magnitude larger than that of χ_{yxx} and χ_{yyy}. (Because of the off-resonance excitation the relation between this ratio and the Eu^{2+} transitions involved is not clear.) Thus, the bulk MD-SHG process in Eq. (1) with a spontaneous magnetization along y correctly describes the SHG data on EuO in Figs. 1 and 2. In particular, no crystallographic contributions to the SHG signal are involved in contrast to the case of EuSe and EuTe films grown on BaF_2 substrates.[16] This is a substantial advantage for any measurements on EuO employing SHG as a probe of the magnetic state.

In order to clarify the microscopic mechanism of the pronounced SHG signal, its spectral dependence in the range of 1.4–3.1 eV is investigated. Figure 1(f) shows the spectra for various SHG components χ_{ijk} at 10 K. A pronounced spectral dependence is observed for χ_{xxy} and χ_{xyx} while the SHG yield for χ_{yyx} and χ_{yxy} is zero across the entire range. The enhancement of the SHG signal below $2\hbar\omega=2.5$ eV coincides with the $4f\rightarrow 5d(t_{2g})$ transitions of the Eu^{2+} ion. For a detailed interpretation of the SHG spectra, we recall that the spin of the electron excited into the $5d$ band is strongly

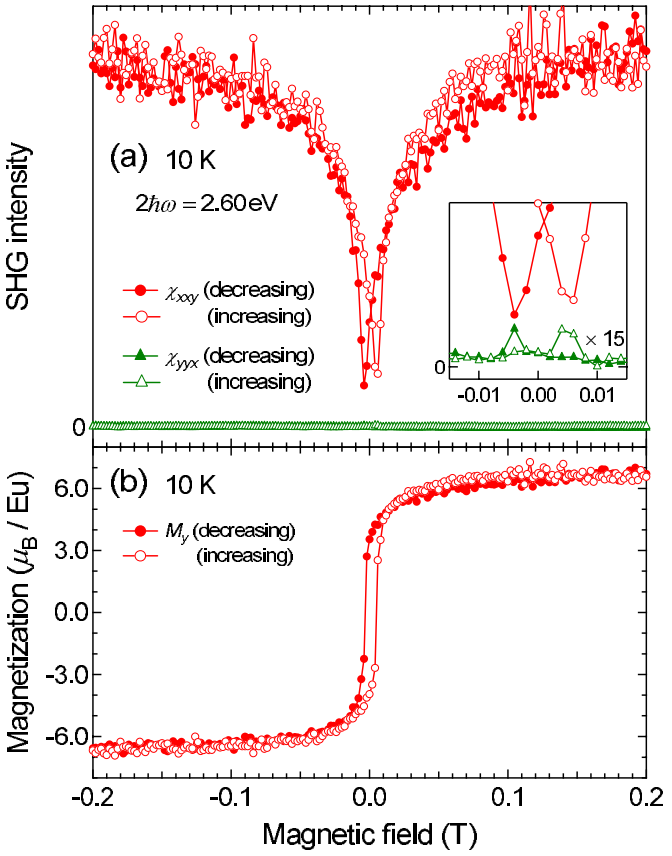

FIG. 3. (Color online) Hysteresis measurements in a magnetic field along y. (a) Magnetic-field dependence of the SHG intensity from χ_{xxy} and χ_{yyx}. Data represented by closed and open symbols were taken with decreasing and increasing field, respectively. The inset shows a magnified view of the region around 0 T. The same relative scales are used in the main panels and the insets. (b) Magnetization (M_y) parallel to the external magnetic field extracted from the data in (a). The vertical scale is derived from the direct magnetization measurements (Ref. 9).

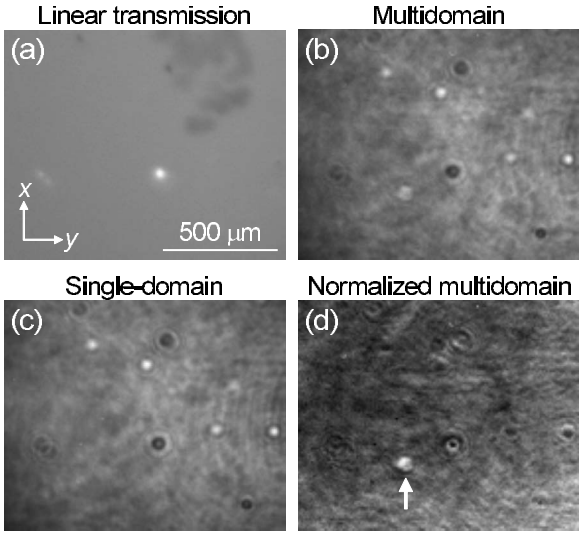

FIG. 4. Imaging of the topography of the crystallographic and magnetic structure of an a-Si/EuO/$YAlO_3$ sample. Black and white correspond to zero and maximum intensity, respectively. (a) Linear transmission image taken with white light from a flash lamp. [(b) and (c)] SHG images for χ_{xxy} at $2\hbar\omega$=1.84 eV in a magnetic field of (b) 0 T and (c) 0.2 T. The brightness of (b) with respect to (c) was enhanced by a factor of 4. (d) Normalized SHG image suppressing spatial inhomogeneities of the SHG yield obtained by dividing the multidomain image in (b) by the single-domain image in (c). The arrow shows a macroscopic single-domain region in the sample after zero-field cooling that is probably stabilized by pinning (see text). The same area is shown in all panels.

coupled to the spin and the orbital momentum of the six remaining electrons in the $4f$ state so that the excitation is more appropriately written as a $4f^7 \rightarrow 4f^6 5d^1(t_{2g})$ transition.

Applying the atomic-coupling scheme proposed earlier,[22,23] the $5d$ states are split by the octahedral crystal field, by the exchange coupling between the spin $S=1/2$ of the $5d^1$ states and the spin $S=3$ of the $4f^6$ states, and by spin-orbit interaction. The latter couples the total spins $S_T=7/2$ or $5/2$ with the orbital momentum $L=3$ of the $4f^6$ states. This leads to the energy levels shown in the inset of Fig. 1(f). In total, three spin-allowed and one spin-forbidden transitions between the J multiplets are possible and located at 1.10, 1.29, 1.54, and 2.08 eV.[22] In the SHG spectra, peaks are observed near 1.5 and 2.0 eV. Accordingly, these structures may be assigned to the two-photon resonant spin-allowed and spin-forbidden transition, respectively. In spite of their lower signal yield, nonlinear optical techniques can be a more sensitive probe of the electronic structures and magnetic states than linear optical techniques because of the involvement of multiple light fields. In the present case, the SHG spectra in Fig. 1(f) reveal rich information including a pronounced polarization dependence and a pronounced peak at the spin-forbidden transition that is not discernible in the weakly structured linear absorption spectrum in Fig. 1(c).

Having analyzed the SHG process in EuO, we now turn to application related issues such as the magnetic hysteresis and the distribution of domains. Figure 3(a) shows the magnetic-field dependence of the SHG intensity at 10 K for χ_{xxy} and χ_{yyx} taken at $2\hbar\omega$=2.60 eV. According to Table I, χ_{xxy} and χ_{yyx} are proportional to the magnetization parallel to the y and x direction, respectively. The SHG intensity for χ_{xxy} varies by 1 order of magnitude with the change in magnetic field along the y direction with different minima in field increasing and decreasing runs. As a result, a butterfly shape is obtained. Considering that the SHG intensity is proportional to the square of the magnetization, the dependence of the magnetization M_y on the applied field H_y is extracted and shown in Fig. 3(b). The result reveals a pronounced hysteresis and reproduces previous "direct" magnetization measurements.[9] The observation of a two orders of magnitude smaller SHG contribution from χ_{yyx} that is forbidden for $M \| y$, indicates that at the coercive field a hitherto unknown finite magnetization M_x *perpendicular* to the applied magnetic field emerges. This may be caused by the formation of closure domains in the multidomain state that is present at the coercive field. In magnetization measurements it is difficult to distinguish this intrinsic contribution from erroneous contributions in a slightly misoriented magnetic field. The SHG measurement is, however, background-free and the fact

that $M_x \neq 0$ is restricted to the vicinity of the coercive field clearly shows that a magnetization component perpendicular to the applied field is inherent to the sample and not due to misalignment.

From the technological viewpoint, it is important to clarify the spatial distribution of the ferromagnetic domains. Here, this distribution is directly probed by spatially resolved SHG images in Fig. 4. First, Fig. 4(a) shows a linear transmission image of the a-Si/EuO/$YAlO_3$ sample at 10 K taken with white light from a flash lamp. Local variations in the brightness are discernible, which indicate local imperfections of the EuO, the a-Si or the substrate. For the same area, Figs. 4(b) and 4(c) show SHG images for χ_{xxy} ($\sim M_y$) at 10 K after zero-field cooling and subsequent to the application of a magnetic field $\mu_0 H_y = 0.2$ T. Although Figs. 4(b) and 4(c) are expected to show multidomain and single-domain states, respectively, no obvious difference except for the brightness is observed between the two SHG images. Therefore, variations in the SHG yield have to be associated with local variations in the sample quality which is confirmed by correlating some of the inhomogeneities to those in the linear transmission image. Domains in Fig. 4(b) would be recognized by the drop of the SHG intensity to zero at the position of the walls between domains with $\pm M_y$.[24] The absence of such structures reveals that the lateral extension of the ferromagnetic domains is at least an order of magnitude below the optical resolution so that such a distribution of domain walls results in a homogeneous decrease in the net SHG intensity.[24] This is confirmed by spatially resolved infrared reflectivity measurements which also point to a subwavelength extension of the ferromagnetic domains in EuO.[25]

More details are revealed by normalizing the SHG intensity of the multidomain image at 0 T to the SHG intensity of the single-domain image at 0.2 T. This suppresses any defect-related variations in the SHG yield and enhances any magnetization-related features. The normalized SHG image in Fig. 4(d) reveals a single feature on the sample with an expansion above the resolution limit. This feature, marked by an arrow, possesses a diameter of 70 μm. The region yields an enhanced SHG intensity in the multidomain image but not in the single-domain image which shows that it corresponds to a single-expanded domain that is already present after zero-field cooling. Apparently, the pinning of this local-expanded domain is caused by inhomogeneities of a different type than those affecting the linear transmission or the SHG yield in Figs. 4(a)–4(c). Figures 3 and 4 thereby demonstrate that SHG probes the magnitude and direction of the magnetization in EuO and also subtle nuances in the spatial distribution of the ferromagnetic domains.

In summary, magnetization-induced optical SHG of the MD type was observed in the centrosymmetric ferromagnetic semiconductor EuO. The spectral dependence of the SHG signal is related to spin-allowed and spin-forbidden transitions between the $4f$ and $5d(t_{2g})$ levels of the Eu^{2+} ion. The polarization of the SHG signal is in agreement with a spontaneous magnetization along the y axis except in the vicinity of the coercive field where an intrinsic component of the magnetization oriented perpendicular to the applied field is detected. Spatially resolved hysteresis measurements revealed that the ferromagnetic domains possess an average extension of <1 μm although pinning effects can stabilize domains that are two orders of magnitude larger.

In contrast to other EuX compounds that were investigated by nonlinear optics, the SHG signal in EuO is purely magnetic, and thus emerges background-free at the Curie temperature. Ferromagnetic order in EuO occurs in the absence of external fields so that the present work constitutes the observation of magnetization-induced bulk SHG in an intrinsic centrosymmetric ferromagnet.

Recent theoretical studies suggest that epitaxial strain can be used to increase T_C of EuO films.[26] In addition, strain-induced ferroelectricity was predicted[27] so that strained ultrathin EuO films may provide a new route toward high-temperature multiferroicity. The present experiments establish a valuable basis for investigations along these lines because SHG is particularly useful for studying the coexistence and interactions of magnetic and electric order.[14,28]

ACKNOWLEDGMENTS

We thank the Deutsche Forschungsgemeinschaft (Grant Nos. SFB 608 and TRR 80) for financial support. M.M. thanks the Alexander von Humboldt Foundation for financial support. D.G.S. gratefully acknowledge support from AFOSR under Grant No. FA9550-10-1-0123.

*matsubara@hiskp.uni-bonn.de

[1] B. T. Matthias, R. M. Bozorth, and J. H. Van Vleck, Phys. Rev. Lett. **7**, 160 (1961).
[2] A. Mauger and C. Godart, Phys. Rep. **141**, 51 (1986).
[3] G. Petrich, S. von Molnár, and T. Penney, Phys. Rev. Lett. **26**, 885 (1971).
[4] M. R. Oliver, J. O. Dimmock, A. L. McWhorter, and T. B. Reed, Phys. Rev. B **5**, 1078 (1972).
[5] Y. Shapira, S. Foner, and T. B. Reed, Phys. Rev. B **8**, 2299 (1973).
[6] H. Ott, S. J. Heise, R. Sutarto, Z. Hu, C. F. Chang, H. H. Hsieh, H.-J. Lin, C. T. Chen, and L. H. Tjeng, Phys. Rev. B **73**, 094407 (2006).
[7] J. Schoenes and P. Wachter, Phys. Rev. B **9**, 3097 (1974).
[8] P. G. Steeneken, L. H. Tjeng, I. Elfimov, G. A. Sawatzky, G. Ghiringhelli, N. B. Brookes, and D.-J. Huang, Phys. Rev. Lett. **88**, 047201 (2002).
[9] A. Schmehl, V. Vaithyanathan, A. Herrnberger, S. Thiel, C. Richter, M. Liberati, T. Heeg, M. Röckerath, L. F. Kourkoutis, S. Mühlbauer, P. Böni, D. A. Muller, Y. Barash, J. Schubert, Y. Idzerda, J. Mannhart, and D. G. Schlom, Nature Mater. **6**, 882 (2007).
[10] M. Arnold and J. Kroha, Phys. Rev. Lett. **100**, 046404 (2008).
[11] R. W. Ulbricht, A. Schmehl, T. Heeg, J. Schubert, and D. G.

Schlom, Appl. Phys. Lett. **93**, 102105 (2008).
[12] K. Y. Ahn and M. W. Shafer, J. Appl. Phys. **41**, 1260 (1970).
[13] K. N. Tu, K. Y. Ahn, and J. C. Suits, IEEE Trans. Magn. **MAG8**, 651 (1972).
[14] For a review, see M. Fiebig, V. V. Pavlov, and R. V. Pisarev, J. Opt. Soc. Am. B **22**, 96 (2005).
[15] *Nonlinear Optics in Metals*, edited by K. H. Bennemann (Clarendon, Oxford, 1998).
[16] B. Kaminski, M. Lafrentz, R. V. Pisarev, D. R. Yakovlev, V. V. Pavlov, V. A. Lukoshkin, A. B. Henriques, G. Springholz, G. Bauer, E. Abramof, P. H. O. Rappl, and M. Bayer, Phys. Rev. Lett. **103**, 057203 (2009).
[17] M. Fiebig, D. Fröhlich, Th. Lottermoser, V. V. Pavlov, R. V. Pisarev, and H.-J. Weber, Phys. Rev. Lett. **87**, 137202 (2001).
[18] R. R. Birss, *Symmetry and Magnetism* (North-Holland, Amsterdam, 1966).
[19] A. B. Henriques, E. Abramof, and P. H. O. Rappl, Phys. Rev. B **80**, 245206 (2009).
[20] G. E. Jellison, Jr. and F. A. Modine, Appl. Phys. Lett. **69**, 371 (1996).
[21] M. J. Freiser, F. Holtzberg, S. Methfessel, G. D. Pettit, M. W. Shafer, and J. C. Suits, Helv. Phys. Acta **41**, 832 (1968).
[22] H.-Y. Wang, J. Schoenes, and E. Kaldis, Helv. Phys. Acta **59**, 102 (1986).
[23] J. Schoenes, J. Alloys Compd. **250**, 627 (1997).
[24] M. Fiebig, D. Fröhlich, Th. Lottermoser, and M. Maat, Phys. Rev. B **66**, 144102 (2002).
[25] S. Kimura, T. Ito, H. Miyazaki, T. Mizuno, T. Iizuka, and T. Takahashi, Phys. Rev. B **78**, 052409 (2008).
[26] N. J. C. Ingle and I. S. Elfimov, Phys. Rev. B **77**, 121202(R) (2008).
[27] E. Bousquet, N. Spaldin, and P. Ghosez, Phys. Rev. Lett. **104**, 037601 (2010).
[28] M. Fiebig, Th. Lottermoser, D. Fröhlich, A. V. Goltsev, and R. V. Pisarev, Nature (London) **419**, 818 (2002).